Hand Gesture Recognition using MYO Armband

Shunzhan He
Key Laboratory of Autonomous Systems and Networked Control
College of Automation Science and Engineering
South China University of Technology
Guangzhou, China
shunzhanhe@gmail.com

Chenguang Yang*
Key Laboratory of Autonomous Systems and Networked Control
College of Automation Science and Engineering
South China University of Technology
Guangzhou, China
cyang@ieee.org

Min Wang
Key Laboratory of Autonomous Systems and Networked Control
College of Automation Science and Engineering
South China University of Technology
Guangzhou, China
auwangmin@scut.edu.cn

Long Cheng
State Key Laboratory of Management and Control for Complex Systems
Institute of Automation
Chinese Academy of Sciences
Beijing, China
long.cheng@ia.ac.cn

Zedong Hu
Key Laboratory of Autonomous Systems and Networked Control
College of Automation Science and Engineering
South China University of Technology
Guangzhou, China
auhz5241@gmail.com

***Abstract*—Surface electromyography (sEMG) is widely used in clinical diagnosis, rehabilitation engineering and human-computer interaction and other fields. In this paper, we use Myo armband to collect sEMG signals. Myo armband can be worn above any elbow of any arm and it can capture the bioelectric signal generated when the arm muscles move. MYO can pass of signals through its low-power Blue-tooth, and its interference is small, which makes the signal quality really good. By collecting the sEMG signals of the upper limb forearm, we extract five eigenvalues in the time domain, and use the BP neural network classification algorithm to realize the recognition of six gestures in this paper. Experimental results show that the use of MYO for gesture recognition can get a very good recognition results, it can accurately identify the six hand movements with the average recognition rate of 93%.**

***Index Terms*—sEMG; Myo Armband; Gesture Recognition; Feature Extraction; BP Neural Network.**

I. INTRODUCTION

The sEMG is a one-dimensional time series signal that is recorded from the muscle surface through the electrode and recorded in the neuromuscular system. Its changes are related to the number of exercise units participating in the activity, the activity mode of the movement unit and the metabolic status. It can accurately reflect muscle activity and functional status in real time and in non-damaged state. It can to a certain extent reflect the activities of neuromuscular, and have important practical value in many fields. Such as neuromuscular disease diagnosis in clinical medicine, ergonomic analysis of muscle work in the field of ergonomics, evaluation of muscle function in the field of rehabilitation medicine, fatigue judgment in sports science, rational analysis of motion techniques, muscle fiber type and anaerobic threshold no damage prediction.

The feature extraction algorithm is critical to the processing of sEMG signals. Until now, a large number of sEMG feature extraction methods have been proposed and applied to scientific research. They mainly include the time domain method, frequency domain method, time-frequency domain method and others. For example, the time domain methods: slope sign changes (SSC), the mean absolute value (MAV), waveform length (WL), root mean square(RMS), number of zero crossings (ZC) [1] and Willison amplitude (WAMP) [6] [20]; the frequency domain methods: mean power frequency (MPF), fast Fourier transform (FFT) [2], median frequency (MF); the time-frequency domain methods: wavelets, wavelet packet transform (WPT) [3] [4]; and some of other methods: cepstral coefficients (CC) [5], sample entropy (ENT) [7], the autoregressive (AR) model parameters [8], and cardinality [9]. Each feature extraction algorithm has its advantages and disadvantages, the specific choice of which algorithm should be based on the actual situation. Time domain method is first applied to EMG signal analysis, because it is easy to extract, and the method is simple. The eigenvalues extracted by the frequency domain method are more stable, making the frequency domain method become the mainstream of EMG signal processing technology, which has been the most widely used. The time-frequency analysis method, represented by wavelet transform, combines the characteristics of time domain and frequency domain.

In this paper, we choose the feature extraction methods in

This work was partially supported by Special Funds for the Cultivation of Guangdong College Students' Scientific and Technological Innovation (Climbing Program Special Funds pdjh2017b0042), National Nature Science Foundation (NSFC) under Grant 61473120, Guangdong Provincial Natural Science Foundation 2014A030313266 and International Science and Technology Collaboration Grant 2015A050502017, Science and Technology Planning Project of Guangzhou 201607010006, State Key Laboratory of Robotics and System (HIT) Grant SKLRS-2017-KF-13, and the Fundamental Research Funds for the Central Universities 2017ZD057.

* Correspond author is C. Yang. Email: cyang@ieee.org

978-1-5386-3524-7/17/$31.00 ©2017 IEEE

[10] [11] to extract features. First, several power spectrum characteristics of the time domain are extracted to reduce computing costs. Later, we estimate the orientation between the extracted power spectrum features from the original sEMG signals and their nonlinear cepstral by employing the cosine similarity. At last, we extract the features from the current analysis windows and the previous windows for robust activity recognition. Experiments show that this feature extraction algorithm is suitable for the requirements of our paper. We will discuss this feature extraction algorithm in the next section.

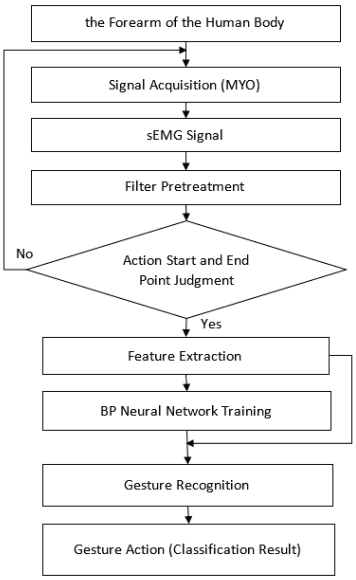

Fig. 1. The flow chart of gesture recognition.

We use Myo armband to collect sEMG signals. Myo Armband was developed by Thalmic Labs in 2014 [12]. MYO is an armband that can be worn on the forearm below the elbow which is controlled by our gestures and movements. The MYO involves five basic gestures: wave left, wave right, double tap, fist and fingers open [12]. Myo armband's application is very extensive, it can be used for mobile phone and personal computer application process control, such as music playback, PPT playback and game control, it can be used for smart cars and aircraft control [13] [14], it can also be used for medical and health, although most of the application in medical health remains at the level of scientific research, such as deaf-mute sign language recognition [15], rehabilitation of stroke patients [16], prosthetic hand control of amputees [17].

As mentioned earlier, Myo armband uses a wide range, but its products come with only five kinds of recognizable gestures, which to some extent limit its promotion. The purpose of this study is based on this, using Myo armband to achieve more recognition of gestures.

The process of gesture recognition can be divided into the following parts: signal acquisition, filter pretreatment, action start and end point judgment, feature extraction, BP neural network training, gesture recognition. These main processing modules will be introduced in detail in the next section. Its flow chart is shown in Fig.1.

II. THEORY AND METHODS

A. Signal Acquisition and Preprocessing

As mentioned earlier, the sEMG signal is collected using Myo armband, which has eight channels, and each channel is equally spaced. Thalmic Labs does not provide a software program that can extract data directly from Myo armband, but it provides a dedicated SDK for the developer. We use the program in [18] to collect data in this article.

Then how do we define MYO's wearing styles? When we collect sEMG data with Myo armband, Myo armband worn on the right hand elbow, place the arm horizontally and fist, fist face up and Myo armbands logo up, as shown in Fig.2.

Fig. 2. The place Myo armband wearing.

In this paper, six new gestures are identified, and these six gestures are set to be: gesture 1, gesture 2, gesture 3, gesture 4, gesture 5, gesture 6. The six gestures are as shown in Fig.3.

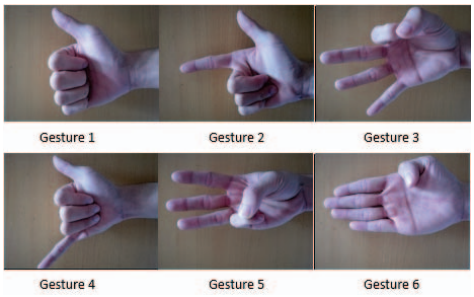

Fig. 3. Six new hand gestures.

The data collected by Myo armband has been processed by amplification and filtering in advance. However, the sEMG signal is a weak bioelectrical signal and in the process of data transmission, noise interference may be introduced. Therefore, before the use of the sEMG signal, it has to be pre-processed again, and the main purpose is to filter out noise. The effective frequency of arm sEMG signals usually concentrate in 45-195 Hz. However, the Myo armband using Bluetooth to transmission data, and as a result, the signal sampling frequency is quiet low, only 200 Hz [19]. So this article uses high-pass digital wave filter to filter the sEMG data, with the cut-off frequency of 45 Hz.

B. Determine the Starting and Ending Point of Action

The method to determine the starting point and the ending point of actions include the threshold method, the neural network method and moving average method. In order to ensure the real-time recognition of gestures, the judgment of the starting and ending points of the action needs to be timely and effective, so the threshold method is adopted. In this paper, Mean Absolute Average (MAV) is used as the judgment criterion of the starting and ending points of the action. For the sEMG signal of the eight channels of Myo armband, we first calculate the MAV of N sampling points for each channel signal using the following formula

$$MAV_i = \frac{1}{N}\sum_{k=1}^{N}|x(k)|, \quad i = 1, 2, 3, \ldots, 8 \tag{1}$$

Adding the MAV of the eight-way signal, and the start and end points of the action are determined by setting the threshold. Although the sEMG signal characteristics of each subject are not exactly the same, the electric potential of the action state is significantly different from the electric potential in the relaxed state. By analyzing the sample datas collected from each subject, it is easy to determine the appropriate threshold for each other. In addition, when the test people and test samples are enough, it is possible to determine a threshold applicable to the vast majority of people. As shown in Fig.4. The formula for seeking the eight-channel MAV is shown below. In fact, when we use it in real, we usually set the threshold a little higher. In this paper, we set the threshold to be 60.

$$MAV = \sum_{i=1}^{8} MAV_i \tag{2}$$

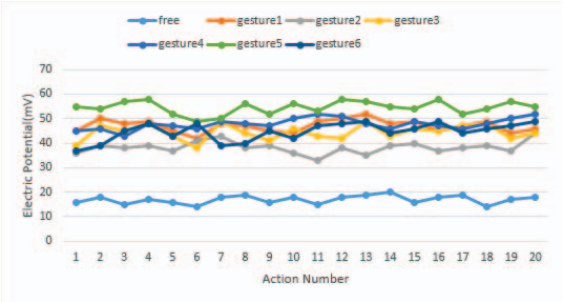

Fig. 4. The sEMG signal comparison chart.

C. Feature Extraction

There are many feature extraction algorithms for surface EMG signals. In this paper, in order to reduce the computational complexity and software real-time considerations, we use a new time domain feature extraction algorithm introduced in [10] and [11]. In order to make it better for Myo armband, this paper has made some minor improvements to the feature extraction algorithm.

The feature extraction algorithm can be mainly divided into three steps. Firstly, by using signal norms and derivatives in [11], [21] and [22], we extract several power spectrum moments of the sEMG signal in the time domain. Secondly, by making use of the cosine similarity, we employ an orientation vector as our desired feature set, which is estimated between the extracted power spectrum features from the original sEMG signals and their non-linear cepstrum. Thirdly, we multiply the features extracted from the current window and the n^{th} previous window to enhance signal characteristics.

First of all, we have to know that as for a sampled sEMG signal version of length N and its sampling frequency is f_s Hz: $x[j]$, with $j = 1, 2, ..., N$, we can employ Discrete Fourier transform (DFT) to express the sEMG trace in a certain period of time as a frequency function $X[k]$ [10] [11]. We mainly employ Parseval's theorem to derive this method. Parseval's theorem is shown in the following formula and it states that the square sum of the function is equal to the square sum of its transformation.

$$\sum_{j=0}^{N-1}|X[j]|^2 = \frac{1}{N}\sum_{k=0}^{N-1}|X[k]X^*[k]| = \sum_{k=0}^{N-1}P[k] \tag{3}$$

We all know that when we derive this method by employing the Fourier transform, the complete frequency description we got is symmetrical for zero frequency. And as a result, it has the same branch that extends to the positive and negative frequencies [23]. Because of the symmetry and we can't get the power spectral density from the time domain directly, and then we have to deal with the whole positive and negative frequencies spectrum. Thus, in order to describe the distribution of frequency domain, according to the definition of a moment m of the n^{th} order of the power spectral density $P[k]$, all odd moments will become zero [23].

$$m_n = \sum_{k=0}^{N-1}k^n P[k] \tag{4}$$

From the equation we know that, when $n = 0$, Parseval's theorem in (3) will be used; and when n is a nonzero number, the time differential characteristics of the Fourier transform will be used. It means that the n^{th} derivative of a discrete time domain function, which is expressed as Δ^n, equal to multiplying the spectrum with the n^{th} power of k.

$$F[\Delta^n x[j]] = k^n X[k] \tag{5}$$

The features extracted by the first step is shown in Fig.5.

Root squared zero order moment $\bar{m}_0$: a feature that describes the frequency domain's total power, or in other words, it indicates the muscle contraction intensity. And it is defined as

$$\bar{m}_0 = \sqrt{\sum_{j=0}^{N-1}x[j]^2} \tag{6}$$

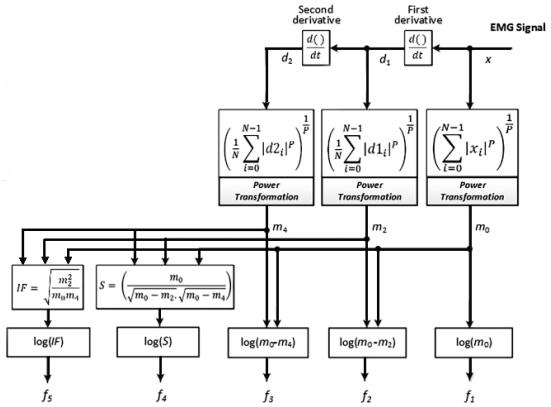

Fig. 5. Block diagram of the proposed feature extraction process(modified from [11]).

Root squared second order moments: according to Hjorth [23], we can consider the second moment as a power, and then a modified spectrum $k^2P[k]$, corresponding to a frequency function

$$\bar{m}_2 = \sqrt{\sum_{k=0}^{N-1} k^2 P[k]} = \sqrt{\frac{1}{N}\sum_{k=0}^{N-1}(kx[k])^2} = \sqrt{\frac{1}{N}\sum_{k=0}^{N-1}(\Delta x[j])^2} \tag{7}$$

Similarly, we can get root squared fourth order moments through the following formula:

$$\bar{m}_4 = \sqrt{\sum_{k=0}^{N-1} k^4 P[k]} = \sqrt{\frac{1}{N}\sum_{k=0}^{N-1}(\Delta^2 x[j])^2} \tag{8}$$

In order to reduce the noise in all feature extraction moments, we normalize the range of $\bar{m}_0$, $\bar{m}_2$, and $\bar{m}_4$ through a power transformation. The power transformation is as follows and λ is empirically set to be 0.1.

$$m_0 = \frac{\bar{m}_0^{\lambda}}{\lambda}, m_2 = \frac{\bar{m}_2^{\lambda}}{\lambda}, m_4 = \frac{\bar{m}_4^{\lambda}}{\lambda} \tag{9}$$

In this case, we employ these variables to define the first three extracted features as follows

$$f_1 = \log(m_0), f_2 = \log(m_0 - m_2), f_3 = \log(m_0 - m_4) \tag{10}$$

Sparseness: this characteristic quantifies how much energy of a certain vector is packed into only a few components. It is defined as follow

$$f_4 = \log\left(\frac{m_0}{\sqrt{m_0 - m_2}\sqrt{m_0 - m_4}}\right) \tag{11}$$

Irregularity Factor (IF): this indicates the ratio of ZC divided by NP. From [24], We know that the number of a random signal's upwardly zero cross points (ZC) and the number of peaks (NP) can be represented by their spectral moments.

$$f_5 = \log\left(\frac{ZC}{NP}\right) = \log\left(\frac{\sqrt{\frac{m_2}{m_0}}}{\sqrt{\frac{m_4}{m_2}}}\right) = \log\left(\frac{m_2}{\sqrt{m_0 m_4}}\right) \tag{12}$$

As can be seen from the schematic diagram of Fig.5, we extract the proposed five features from each sEMG record x at first and as a result, we form a vector $a = [a_1, a_2, a_3, a_4, a_5]$. Later, we extracted an additional feature vector from a logarithmically scaled version, and it is denoted as $b = [b_1, b_2, b_3, b_4, b_5]$. The logarithmically scaled version is defined as follow

$$y = \log(x^2 + 1) \tag{13}$$

Then we get two feature vectors in all: one is a which is from the original sEMG signal, the other is b which is from a nonlinearly scaled version of the sEMG signal. Both of them include 5 elements.

Then we go to the second step, we employ a cosine similarity measure to get the two vectors' orientation. And the definition of the cosine similarity measure is as follow

$$f_i = \frac{-2a_i b_i}{a_i^2 + b^2}, \quad i = 1, 2, \ldots, 5 \tag{14}$$

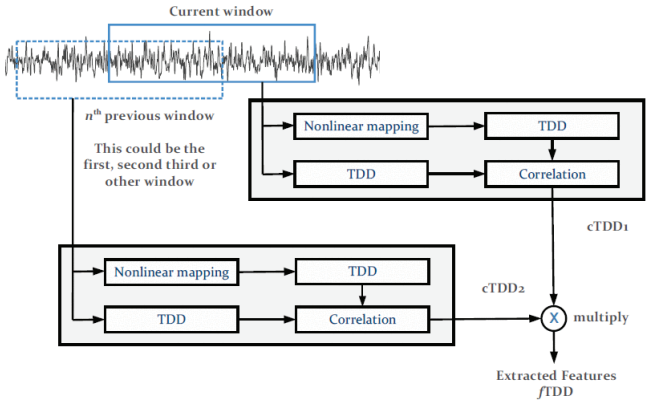

Fig. 6. The block diagram of the complete feature extraction process(modified from [11]).

In the end, we multiply the features extracted from the current window and the n^{th} previous window. In this way, the correlation values will boost when the previous window features and the current window features are from the same classes; and the correlation values will diminish when the features of the current window and the previous window are from the non-similar classes [11]. The block diagram of Fig.6 shows the whole feature extraction process. In this paper, we use the 3^{rd} previous window to extract features and the experimental results perform well.

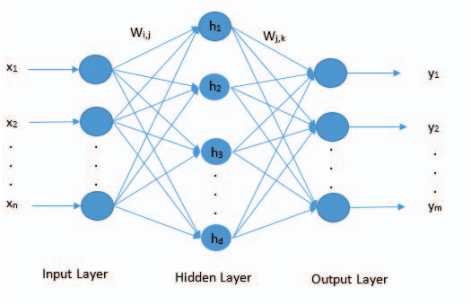

Fig. 7. The structure of three layer BP neural network.

D. BP Neural Network

In this paper, a three-tier BP neural network with supervised learning is used as a classifier. The basic principle of BP neural network is that the input signal x_i is output to the output node through the intermediate node (hidden layer), and the output signal y_m is generated by non-linear transformation. The network training samples includes the input vector x and the expected output vector y. The deviation between the output value y and the expected output Y of the network, make the error decreases in the gradient direction by adjusting the join strength $W_{i,j}$ of the input node and the hidden node, the join strength $W_{j,k}$ of the hidden node and the output node and the threshold. After a number of training, we use the minimum error to determine the network parameters (weights and thresholds), and training is stopped. At this point, according to the input information for similar samples, the trained neural network can self-process and output information with smallest error through non-linear conversion.

In this paper, we use hyperbolic tangent sigmoid transfer function as the activation function. And it is as follow:

$$f(x) = \frac{1 + e^x}{1 - e^x} \tag{15}$$

Learning rate and the number of hidden nodes are important parameters for BP neural network. Learning rate is generally selected as 0.01-0.8, if it is too large, it will lead to the system of instability, and if it is too small, it will lead to convergence too slow, and even requires a longer training time. Through repeated tests, the final determination of the learning rate is 0.2. As for the number of hidden nodes, when the hidden nodes are too many, it will make the learning time become longer, and even make the system can't converge; and when the hidden points are too small, the network fault tolerance is poor. In this paper, through the number of attempts, we finally find a suitable number of hidden nodes for our model.

BP algorithm has some limitations, it uses the gradient descent method, which may lead to the results converge to the local minimum, and the training time is longer. In order to speed up the training speed and to avoid falling into the local minimum, this paper uses the momentum factor method to improve the BP algorithm. The basic idea of the momentum factor method is to add a value that is proportional to the change in the previous weight on each change in weight on the basis of reverse propagation, and produce new weight changes according to the reverse propagation method.

TABLE I
THE RESULT OF THE FIRST TESTER

Gesture	1	2	3	4	5	6	unknow
1	95.76%	0.84%	0	0	0	0.03%	3.37%
2	2.03%	94.26%	0	0.43%	0	0	3.28%
3	0	0	93.65%	0.25%	0.58%	1.04%	4.48%
4	1.07%	0	0	93.77%	0	0	5.16%
5	0	0	0	0	98.90%	0	1.10%
6	0.71%	0	0	0	1.01%	91.50%	6.78%

TABLE II
THE RESULT OF THE SECOND TESTER

Gesture	1	2	3	4	5	6	unknow
1	91.49%	0	0	0	3.43%	0	5.08%
2	0	95.21%	0	0	0	0.10%	4.69%
3	0	0	88.48%	0	0	0.84%	10.68%
4	1.68%	0	0	95.94%	0	0	2.38%
5	0	0	0.77%	0	98.43%	0.12%	0.68%
6	0	0	7.86%	0	0	85.08%	7.06%

III. EXPERIMENTS AND RESULTS

From the previous analysis and calculation we can see that we get a total of 40 inputs for BP neural network. Through several tests, we found that the signal quality of some channels is poor, and the characteristics of these channels are not obvious. Through repeated trials and comparisons, we finally decided to remove the 5^{th} and 6^{th} channels' signals and get 30 inputs at last. It can be seen that BP neural network contains 30 input nodes and 6 output nodes.

We have a total of five testers, we make a tester to repeat the six gestures for 30 times as a training sample, and repeat the six gestures for 50 times as a test sample. After filtering, we extract the signal characteristics of the train sample and put it into the training of BP neural network, and then use the signal characteristics extracted from the test sample to test the training results. The other four testers tested in the same way, and eventually found that there are some differences between the results of the different testers, but the overall gesture recognition rate is higher than 93%.

Table 1 and Table 2 are the results of the gestures classified by two different testers. It can be found that there are some individual differences in the extracted sEMG signals. We draw a conclusion that some people have good electromyography (low noise) and others' signal quality is slightly worse.

Table 3 shows the average gesture classification results for five testers, with an average recognition rate of 93.43% for the six gestures. As can be seen from the table, there is a difference

TABLE III
AVERAGE RECOGNITION RATE OF ALL THE TESTERS

Gesture	1	2	3	4	5	6	unknow
1	93.63%	0.42%	0	0	1.22%	0.02%	4.71%
2	1.02%	94.74%	0	0.22%	0	0	4.02%
3	0	0	90.05%	0.13%	0.29%	0.37%	9.16%
4	1.38%	0	0	94.86%	0	0	3.76%
5	0	0	0.39%	0	98.67%	0.06%	0.88%
6	0.36%	0	3.43%	0	0.55%	88.65%	7.01%

in the recognition rate of the six gestures, for example, the recognition rate of the gesture 5 is high and the recognition rate of the gesture 6 is a little low. In fact, through the experiment we found that the gestures which is relatively strong signal, its recognition rate is often higher, such as Myo armband's own gestures wave left and wave right, their recognition rate is very high.

IV. DISCUSSION AND CONCLUSION

The results of the existing experiments show that the classification results will be better if the sEMG signal is stronger. However, when the two gestures are similar, their sEMG signals are also similar. If training the two gestures in the BP neural network at the same time, the recognition rate of both gestures will reduce. Experiments also show that using this feature extraction algorithm and BP neural network, we can do the number of gesture recognition maintained at 6-8 at this stage (when including the gestures of wave left and wave right, we can identify 8 gestures at all). On this basis, when increasing gestures, the recognition rate will drop sharply. The main reason is that the hand gestures of strong signals are limited, increasing the number will lead to more similar gestures. The initial goal of this study was to make gestures recognition for the vast majority of people, as in the case of Myo armband's own gestures. But as said on the Thalmic Labs official website, to make a general type of gesture recognition requires a large number of individual data samples. Because for the same gesture, there are some differences between the sEMG signals extracting from different individuals, and sometimes the differences will even be great.

The next job for us is to ensure that the gesture recognition method can be applied to Myo armband in real time and to maintain a high recognition rate. By improving the algorithm, increase the gesture recognition number of Myo armband. If the experimental conditions permit, try to do general-purpose gesture recognition, training out a model which is suitable for the vast majority of people, just like Myo armband's own five gestures.

REFERENCES

[1] B. Hudgins, P. Parker and R. N. Scott, "A new strategy for multifunction myoelectric control," in IEEE Transactions on Biomedical Engineering, vol. 40, no. 1, pp. 82-94, Jan. 1993.

[2] L. Q. Zhang, R. Shiavi, M. A. Hunt and J. J. J. Chen, "Clustering analysis and pattern discrimination of EMG linear envelopes," in IEEE Transactions on Biomedical Engineering, vol. 38, no. 8, pp. 777-784, Aug. 1991.

[3] Xin Guo, Peng Yang, Ying Li and Wei-Li Yan, "The SEMG analysis for the lower limb prosthesis using wavelet transformation," The 26th Annual International Conference of the IEEE Engineering in Medicine and Biology Society, San Francisco, CA, 2004, pp. 341-344.

[4] S. Karlsson, Jun Yu and M. Akay, "Enhancement of spectral analysis of myoelectric signals during static contractions using wavelet methods," in IEEE Transactions on Biomedical Engineering, vol. 46, no. 6, pp. 670-684, June 1999.

[5] Chih-Lung Lin et al. , "Improved EMG pattern recognition using the distribution plot of cepstrum," Proceedings of the 20th Annual International Conference of the IEEE Engineering in Medicine and Biology Society. Vol. 20 Biomedical Engineering Towards the Year 2000 and Beyond (Cat. No. 98CH36286), Hong Kong, 1998, pp. 2620-2622 vol. 5.

[6] A. Phinyomark, G. Chujit, P. Phukpattaranont, C. Limsakul and Huosheng Hu, "A preliminary study assessing time-domain EMG features of classifying exercises in preventing falls in the elderly," 2012 9th International Conference on Electrical Engineering/Electronics, Computer, Telecommunications and Information Technology, Phetchaburi, 2012, pp. 1-4.

[7] D. Rivela, A. Scannella, E. E. Pavan, C. A. Frigo, P. Belluco and G. Gini, "Processing of surface EMG through pattern recognition techniques aimed at classifying shoulder joint movements," 2015 37th Annual International Conference of the IEEE Engineering in Medicine and Biology Society (EMBC), Milan, 2015, pp. 2107-2110.

[8] Han-Pang Huang, Yi-Hung Liu, Li-Wei Liu and Chin-Shin Wong, "EMG classification for prehensile postures using cascaded architecture of neural networks with self-organizing maps," 2003 IEEE International Conference on Robotics and Automation (Cat. No. 03CH37422), 2003, pp. 1497-1502 vol. 1.

[9] M. Ortiz-Catalan, "Cardinality as a Highly Descriptive Feature in Myoelectric Pattern Recognition for Decoding Motor Volition," Frontiers in Neuroscience, vol. 9, 2015.

[10] A. H. Al-Timemy, R. N. Khushaba, G. Bugmann and J. Escudero, "Improving the Performance Against Force Variation of EMG Controlled Multifunctional Upper-Limb Prostheses for Transradial Amputees," in IEEE Transactions on Neural Systems and Rehabilitation Engineering, vol. 24, no. 6, pp. 650-661, June 2016.

[11] R. N. Khushaba, A. Al-Ani, A. Al-Timemy and A. Al-Jumaily, "A fusion of time-domain descriptors for improved myoelectric hand control," 2016 IEEE Symposium Series on Computational Intelligence (SSCI), Athens, 2016, pp. 1-6.

[12] S. Rawat, S. Vats and P. Kumar, "Evaluating and exploring the MYO ARMBAND," 2016 International Conference System Modeling and Advancement in Research Trends (SMART), Moradabad, 2016, pp. 115-120.

[13] Thalmic Labs. MyoCraft Fly your Parrot AR. Drone 2.0 with AutoFlight. http://developerblog.myo.com/myocraft-fly-your-parrot-ardrone-2-0-with-autoflight/, April, 2015.

[14] Thalmic Labs. Flying Drones with MyoPilot. http://developerblog.myo.com/flying-drones-with-myopilot/, July, 2015.

[15] J. G. Abreu, J. M. Teixeira, L. S. Figueiredo and V. Teichrieb, "Evaluating Sign Language Recognition Using the Myo Armband," 2016 XVIII Symposium on Virtual and Augmented Reality (SVR), Gramado, 2016, pp. 64-70.

[16] A. Hidayat, Z. Arief and H. Yuniarti, "LOVETT scalling with MYO armband for monitoring finger muscles therapy of post-stroke people," 2016 International Electronics Symposium (IES), Denpasar, 2016, pp. 66-70.

[17] Thalmic Labs. Meet the Man With a Myo-Controlled Robotic Arm. http://developerblog.myo.com/meet-the-man-with-a-myo-controlled-robotic-arm/, November, 2015.

[18] Thalmic Labs. MyoCraft: Logging IMU and Raw EMG Data. http://developerblog.myo.com/myocraft-logging-imu-and-raw-emg-data/, March, 2015.

[19] H. J. Kim, Y. S. Lee and D. Kim, "Arm Motion Estimation Algorithm Using MYO Armband," 2017 First IEEE International Conference on Robotic Computing (IRC), Taichung, 2017, pp. 376-381.

[20] Z. Ju, G. Ouyang, M. Wilamowska-Korsak and H. Liu, "Surface EMG Based Hand Manipulation Identification Via Nonlinear Feature Extraction and Classification," in IEEE Sensors Journal, vol. 13, no. 9, pp. 3302-3311, Sept. 2013.

[21] R. N. Khushaba, Lei Shi and S. Kodagoda, "Time-dependent spectral features for limb position invariant myoelectric pattern recognition," 2012 International Symposium on Communications and Information Technologies (ISCIT), Gold Coast, QLD, 2012, pp. 1015-1020.

[22] E. Juuso, S. Lahdelma, "Signal processing and feature extraction using real order derivatives and generalised norm. Part 1: Methodology," Vib. J., vol. 1, no. 2, pp. 46-53, 2011.

[23] B. Hjorth, "EEG analysis based on time domain properties," Electroencephalography and Clinical Neurophysiology, vol. 29, pp. 306-310, 1970.

[24] R. N. Khushaba, M. Takruri, J. V. Miro, S. Kodagoda, "Towards limb position invariant myoelectric pattern recognition using time-dependent spectral features," Neural Networks, vol. 55, pp. 42-58, 2014.